

# Directional wave parameter interpretation and related statistical uncertainties

## Interprétation des paramètres de la houle directionnelle et incertitudes statistiques relatives à celle-ci

CARL TRYGVE STANSBERG, *Norwegian Marine Technology Research Institute A.S. (MARINTEK), N-7450 Trondheim, Norway*

### ABSTRACT

The theoretical background and the interpretation of directional parameters derived from the first two complex Fourier coefficients of the directional distribution, or corresponding circular moments, is reviewed. It is found that for a four-parameter bi-modal spectrum type, cases with small secondary peaks can be clearly distinguished from cases with almost equal peaks. Some other relationships are also noticed. A simple and robust parametric estimation method is suggested and discussed. Statistical errors in parameters estimated from finite time series are investigated. Through a numerical case study, the resulting variability in directional parameters is illustrated. For the actual, limited set of conditions included in the case study, the main structures of the spectral characteristics are reasonably well identified from a given set of records, with a limited level of accuracy given by the variability.

### RÉSUMÉ

On examine le fondement théorique et l'interprétation des paramètres directionnels déduits des deux premiers coefficients de Fourier complexes de la distribution directionnelle, ou des moments circulaires correspondants. Il apparaît que pour un type de spectre bi-modal à quatre paramètres, les cas avec petits pics secondaires se distinguent clairement des cas avec pics presque égaux. Quelques autres relations sont également notées. On suggère et discute une méthode simple et robuste d'estimation des paramètres. On étudie les erreurs statistiques dans les paramètres estimés à partir de séries temporelles finies. La variabilité des paramètres directionnels qui en résulte est illustrée par une étude de cas numérique. En réalité, l'ensemble de conditions incluses dans l'étude de cas étant restreint, les structures principales des caractéristiques spectrales sont raisonnablement bien identifiées à partir d'un ensemble donné d'enregistrements, avec un niveau limité de certitude donné par la variabilité.

### 1. Introduction

The role of multidirectional wave effects in the analysis of off-shore and coastal structures has become increasingly important during the recent years. This may have several reasons. Structural and motion responses are in most cases sensitive to whether waves are unidirectional or not. The essential information here is not only the mean direction and the total amount of directional spreading, but also e.g. whether the spectrum is two-peaked vs. single-peaked. At the same time, more and more field data are becoming available for use in design, and the level of accuracy is also improved. In parallel with this, an increasing number of model testing laboratories are now being equipped with directional wave facilities. Still, compared to the unidirectional case, the modelling, interpretation and use of directional waves is certainly more challenging and complex, for the wave modeller as well as for the end user, and the level of field data basis should be further improved. Standard procedures taking into account directionality are not yet firmly established, although activities are being undertaken to reach a common understanding (Briggs, 1997). Thus it is still some way to go before multidirectional waves are used as frequently as the unidirectional. One of several problems encountered is the establishment of robust and useful parameters for standard use covering a variety of situations in the field as well as in laboratory measurements. The accuracy and possible errors of directional estimates is also a matter of investigation.

The problem addressed in this study is how to derive and interpret

useful estimates of directional spectrum parameters, from available time series of certain water wave surface properties commonly obtained from standard measuring devices. In particular, the estimation of parameters describing the possible bi-modal properties of the spectrum is addressed. The sensitivity to statistical variability is also illustrated through a set of numerical simulation examples, since finite records of random processes will always introduce statistical errors in the estimates. We shall restrict ourselves to the type of information that can be transformed into estimates of the first complex circular moments of the directional spectrum. More precisely, the first four real-valued Fourier coefficients are estimated. This corresponds, in principle, to what can be obtained with the traditional pitch-and-roll buoys, or other measuring devices giving equivalent information such as single-point 2D-velocity-&-elevation probes or simple wave gage arrays. The limitations in what can possibly be estimated (the directional resolution) from this set of coefficients is also addressed. The theory of directional data analysis has been treated earlier by a large number of authors through the last decades. For descriptions of the circular moments and the related Fourier coefficients of the directional distributions, see Longuet-Higgins et. al. (1963), Borgman (1969), Mardia (1972) and Kuik et. al. (1988). A review study including some basic definitions and formulations of directional analysis is given by Benoit et. al. (1997), while a set of frequently used parameters has been listed and briefly discussed by Frigaard et. al. (1997). A description of field data analysis is given in Hashimoto (1997). Another review, dealing with directional distributions, has been recently made by Krogstad &

Revision received April 17, 2002. Open for discussion till October 31, 2002.

Barstow (1999). Today, one of the most commonly used estimation methods is the Maximum Entropy Method (MEM), of which there are several types (Kobune & Hashimoto, 1986; Nwogu et. al., 1987; Nwogu, 1989). The MEM analysis is usually considered as a non-parametric one, with the resulting estimate expressed explicitly as a spectrum, based on an assumption of “maximum entropy” in the system. In the present analysis, however, the idea is to consider the limited set of model-free directional parameters that are actually available directly from e.g. pitch- and roll buoy measurements (without any assumptions made), and how they can be interpreted for bimodality analysis. Some previous results and parameters from the literature will be reviewed and further discussed. It is not the intention to discuss directional analysis in general, which is a very broad subject, but rather to focus on the main parameters describing the mean direction, the spreading and possible bimodality. A 4-parameter bimodal spectrum model is applied for illustration of the different spectrum properties. As one result, a possible approach for a simple and robust bimodal parametric method is suggested. The final development of such a procedure is, however, outside the scope of this paper. The related statistical variability in the estimates from a random sea is also investigated, through a numerical case study with random Monte Carlo simulations. The simulation study makes use of recent works in Stansberg (1998a, 1998b).

## 2. Directional parameters derived from circular moments

*Background: Circular moments and model-free directional parameters*

The background theory of this analysis has been treated by several authors, of which we here mention Borgman (1969), Mardia (1972) and Kuik et. al. (1988). In our present formulation, we make use of some of their main relations and definitions as a basis for the further analysis.

Assume that for a given wave frequency  $f$ , we can write a given, normalized directional energy distribution  $D(\theta)$  in terms of its complex Fourier coefficients  $C_m$ :

$$D(\theta) = (1/2\pi) \sum_{m=-\infty}^{+\infty} C_m \exp(j m \theta) \quad (1)$$

The inverse transform expressing  $C_m$  in terms of  $D(\theta)$  is then:

$$C_m \equiv \int_0^{2\pi} D(\theta) \exp(-j m \theta) d\theta \equiv a_m + j b_m \equiv |C_m| \exp(j \phi_m) \quad (1a)$$

where  $a_m$  and  $b_m$  are the real and imaginary parts, respectively, and  $j$  is the imaginary unit  $\sqrt{-1}$ . For simplicity, we have omitted the frequency in the expressions, since the analysis discussed is carried out at a given, but auxiliary frequency  $f$ .

Let the mean wave direction  $\theta_0$  be defined equal to the phase angle of the first complex coefficient  $C_1$ :

$$\theta_0 \equiv \arg(C_1) \equiv \arctan(b_1/a_1) \equiv \phi_1 \quad (2)$$

Phase angles and directions are here given in radians. (Degree units are also used in later sections, but in those cases it will be specified).

Then we can re-write the expressions in terms of centred Fourier coefficients, through rotating the co-ordinate system by an angle  $\theta_0$ :

$$C_{c,m} \equiv C_m \cdot \exp(-j m \theta_0) \equiv p_m + j q_m \equiv |C_m| \exp(j \phi_{c,m}) \quad (3)$$

where  $p_m$  and  $q_m$  are the centred real-valued Fourier coefficients. See Figure 1. (Notice that  $p_1 \equiv |C_1|$ ). The corresponding central circular moments  $\eta_{m,n}$  can be written (Kuik et. al., 1988):

$$\eta_{m,n} = 2^n \int_0^{2\pi} \sin^m(\theta - \theta_0) \sin^n\{(\theta - \theta_0)/2\} D(\theta) d\theta \quad (4)$$

Now we consider only on the first two complex coefficients,  $C_1$  and  $C_2$  (or  $C_{c,1}$  and  $C_{c,2}$  plus  $\theta_0$ ), which are the coefficients that can be estimated from “Single-Location-Triple-sensor” (SLT) type of devices such as pitch-roll buoys. Also wave gage arrays can be used to estimate  $C_1$  and  $C_2$  (and higher orders as well). The connection between these underlying coefficients and those parameters describing the physical directional spectrum is reviewed in the following.

From eq.(4), the four moments  $\eta_{0,2}$ ,  $\eta_{2,0}$ ,  $\eta_{1,2}$  and  $\eta_{0,4}$  are used to formulate model-free expressions for the width (standard deviation), the skewness and the kurtosis, respectively, of the directional distribution  $D(\theta)$ :

$$\left. \begin{aligned} \text{stand. dev.: } \sigma &= (\eta_{0,2})^{1/2} = [2(1-p_1)]^{1/2} \\ &\quad (\text{in radians}) \\ \text{skewness: } \gamma &= \eta_{1,2} / (\eta_{2,0})^{3/2} = -q_2 / [0.5(1-p_2)]^{3/2} \\ &\quad (\text{dimensionless}) \\ \text{kurtosis: } \delta &= \eta_{0,4} / \sigma^4 = (6-8p_1+2p_2) / \sigma^4 \\ &\quad (\text{---}) \end{aligned} \right\} \quad (5)$$

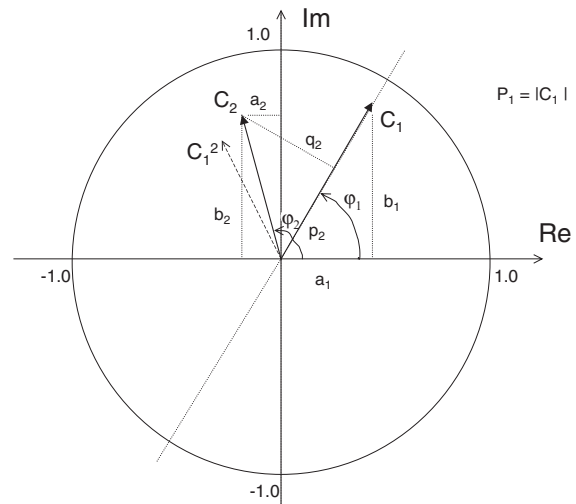


Fig. 1 Illustration of the complex Fourier coefficients  $C_1$  and  $C_2$ . (Additional comment:  $p_2$  and  $q_2$  are the real and imaginary parts, respectively, of  $C_2$ , in the system rotated to  $C_1$ ).

In addition, we have the mean direction  $\theta_0$  defined through eq. 2. These four relations imply that in addition to the two “primary” properties – the mean direction and the directional spreading obtained from  $C_1$  – we have two additional parameters – the skewness and the kurtosis. They indicate the possible deviation from a uni-modal Gaussian-shaped distribution (which is quite similar to the  $\cos^{2s}(\theta)$  type), as seen from the following: Kuik et. al. (1988) have presented a detailed analysis of the problem, showing that the circular parameters from the above definitions have properties similar to their line equivalents, especially for narrow distributions (that is, when  $\sigma$  is small such that  $\sin\sigma \approx \sigma$ ). Thus  $\gamma$  is zero for a symmetrical distribution, and  $\delta$  is expected to be around 3.0 for a Gaussian-shaped distribution. From a given set of the four directional parameters  $\theta_0$ ,  $\sigma$ ,  $\gamma$  and  $\delta$  we are then, in principle, able to describe the rough structure of the spectrum. However, estimates are not unique in the finer details, for which coefficients (moments) of higher order  $m$  are needed as additional input. In the present study we restrict ourselves to the above parameters only. A brief discussion of their properties is given below.

Notice that there are various Gaussian distribution formulations in use for directional spectra, including the “conventional” linear distribution as well as the circular Gaussian distribution defined e.g. by Borgman (1967). Strictly speaking, the use of circular distributions may be considered more consistent with the use of circular moments etc. However, for simplicity, and since various descriptions in the literature actually use the linear Gaussian model, we shall assume the linear one. This makes no difference for narrow spectra, while the truncation of spectral tails outside 0 and  $2\pi$  may be observable for broad spectra since the linear Gaussian model theoretically has no tail limit. Thus for a broad linear Gaussian-shaped spectrum the kurtosis should, e.g., be expected to be slightly lower than 3.0.

Since  $D(\theta)$  is always positive, implying that its complex Fourier coefficients form a positive semi-definite sequence, there exists a restriction on  $p_2$  conditioned on  $p_1$  and  $q_2$  (Mardia, 1972, and Kuik et. al., 1988):

$$1 - p_2^2 - q_2^2 - 2p_1^2(1 - p_1^2) \geq 0 \quad (6)$$

This can alternatively be expressed through the complex Fourier coefficients  $C_2$  and  $C_1$  (Krogstad & Barstow, 1999), as also illustrated in Figure 1:

$$|C_2 - C_1^2| < 1 - |C_1|^2 \quad (6a)$$

Thus  $C_2$  can take values only within a circle with radius  $1 - |C_1|^2$  around the complex value  $C_1^2$ . The actual location of  $C_2$ , given  $C_1$ , is determined by the shape of  $D(\theta)$ , and is uniquely given by the four directional parameters from eqs. (2) and (5) (since  $C_2$  and  $C_1$  in fact represent four real values). If the phase angle  $\varphi_2 \neq 2\varphi_1$ , the spectrum is asymmetric. Notice that the center of the circle,  $C_2 = C_1^2$ , corresponds to the “Maximum Entropy” estimate if only  $C_1$  is known (according to the definition used in Burg, 1975), while  $\cos^{2s}(\theta)$  – or Gaussian-shaped type of spectra result in

smaller values ( $|C_2| \approx |C_1|^4$ ). To estimate quantitative and useful directional information from the coefficients is, except from the mean and the spreading, in general not straightforward. This is further discussed in the following sections, with particular focus on bimodal spectra.

### Bimodal spectra

Various criteria have been suggested for the identification of multiple peaks in directional spectra from the first circular Fourier coefficients (or similar parameters). Besnard & Benoit (1994) have investigated several of these criteria. One of them, proposed by Kuik et. al. (1988), is making use of an x-y plot between the skewness  $\gamma$  and the kurtosis  $\delta$ ; see Figure 2. In the referred work, it is distinguished between two areas in this plot: an upper area indicating unimodal or symmetric spectra and a lower area indicating bimodal spectra. In the following analysis, a similar approach is investigated through examples with the following specific two-peaked linear Gaussian spectrum model:

$$D(\theta) = [A_I / \sqrt{(2\pi)\sigma_I}] \exp[-(\theta - \theta_I)^2 / (2\sigma_I^2)] + [A_{II} / \sqrt{(2\pi)\sigma_{II}}] \exp[-(\theta - \theta_{II})^2 / (2\sigma_{II}^2)] \quad (7)$$

where  $A_I + A_{II} = 1$ . As seen from the expression, this model with  $\sigma_I = \sigma_{II}$  is a special, simplified version of a more general one with two different standard deviations for the two peaks:  $\sigma_I$  &  $\sigma_{II}$ . It has been chosen for this example since it only has 4 variables, which is the same number as in the estimates from the previous section. A similar 4-parameter model was used by Van Heteren (1983). With 5 variables, there would have been 1 unknown, see for example Benoit (1992), Benoit et. al. (1997). In any case, the present model gives a reasonable picture of the possible existence

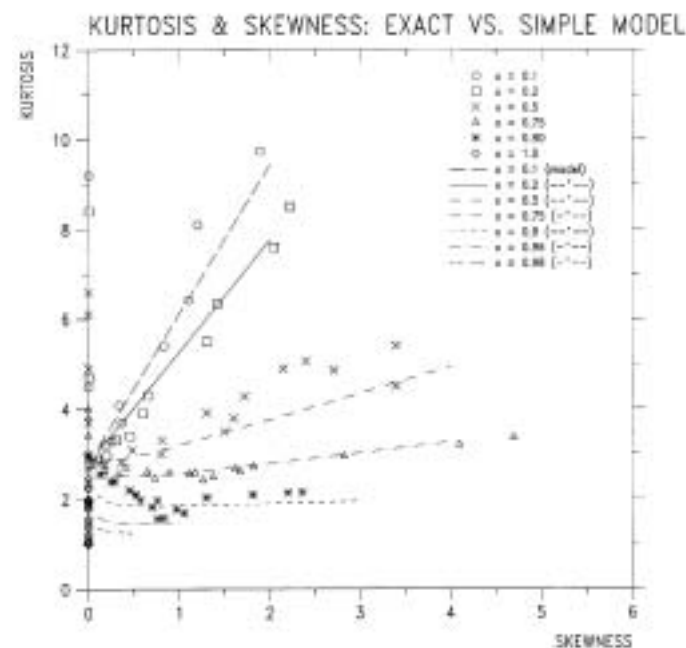


Fig. 2 The skewness-kurtosis domain. Values from 4-parameter model compared to empirical analytical formula.

of a two-peaked spectrum, but one must remember its limitations in the interpretations. The centred complex Fourier coefficients can be easily expressed analytically, combining eqs. (7), (1) & (3):

$$C_{c,m} \equiv p_m + jq_m = \exp[-\frac{1}{2}(m\sigma_1)^2 - jm\theta_0] \cdot [A_I \exp(jm\theta_I) + A_{II} \exp(jm\theta_{II})] \quad (8)$$

with  $\theta_0$  found from eq.(2). With eq.(8) we can directly calculate the directional skewness  $\gamma$  and kurtosis  $\delta$  from eq. (5). Results from this, done for a selected group of combinations between  $(A_{II} / A_I)$ ,  $\Delta\theta = (\theta_{II} - \theta_I)$  and  $\sigma_1$ , are shown in Figure 2. Rather than using the ratio  $(A_{II} / A_I)$  in the analysis, we have chosen to use the parameter

$$x \equiv 4 A_I \cdot A_{II}$$

This works regardless of whether  $A_I$  or  $A_{II}$  is the largest, and it is zero for unimodal and 1.0 for perfectly symmetric two-peaked spectra. Some of the actual spectra  $D(\theta)$  represented in Figure 2 are shown in Figure 3 for illustration. Notice that the actual model

also includes asymmetric spectra which are apparently unimodal. Figure 2 shows some interesting results. While the definition from Kuik et. al. (1988) separates bimodal and unimodal /symmetric spectra into two distinct parts of the  $\gamma - \delta$  domain, our results shows that bimodal spectra are possible all over the range. The apparent discrepancy certainly has to do with the definition of bi-modality. In our application we have included also small values of  $x$  within the “bimodal” definition, while in the “old” definition, probably only cases with larger  $x$ -values were covered (that is, not including cases with rather small secondary peaks). Furthermore, we also see a systematic behaviour in the dependency of  $x$ : Any point-pair  $(\gamma, \delta)$ , and its gradient given by  $(\delta - 2.80) / \gamma$ , seems to be approximately given by  $x$ . Thus for a given skewness value, the kurtosis is highest when the secondary peak is small ( $x$  is small). On the other hand, when the two peaks are about the same size, the kurtosis is low. The lowest kurtosis, 1.0, is obtained with two exactly equal peaks with infinitesimal width (two equal unidirectional wave trains travelling in different directions). This corresponds to one of the limiting cases given by eq.(6a), see the discussion by Krogstad & Barstow (1999). We have found empirically that the following analytical relationship, which is also indicated in Figure 2, corresponds approxi-

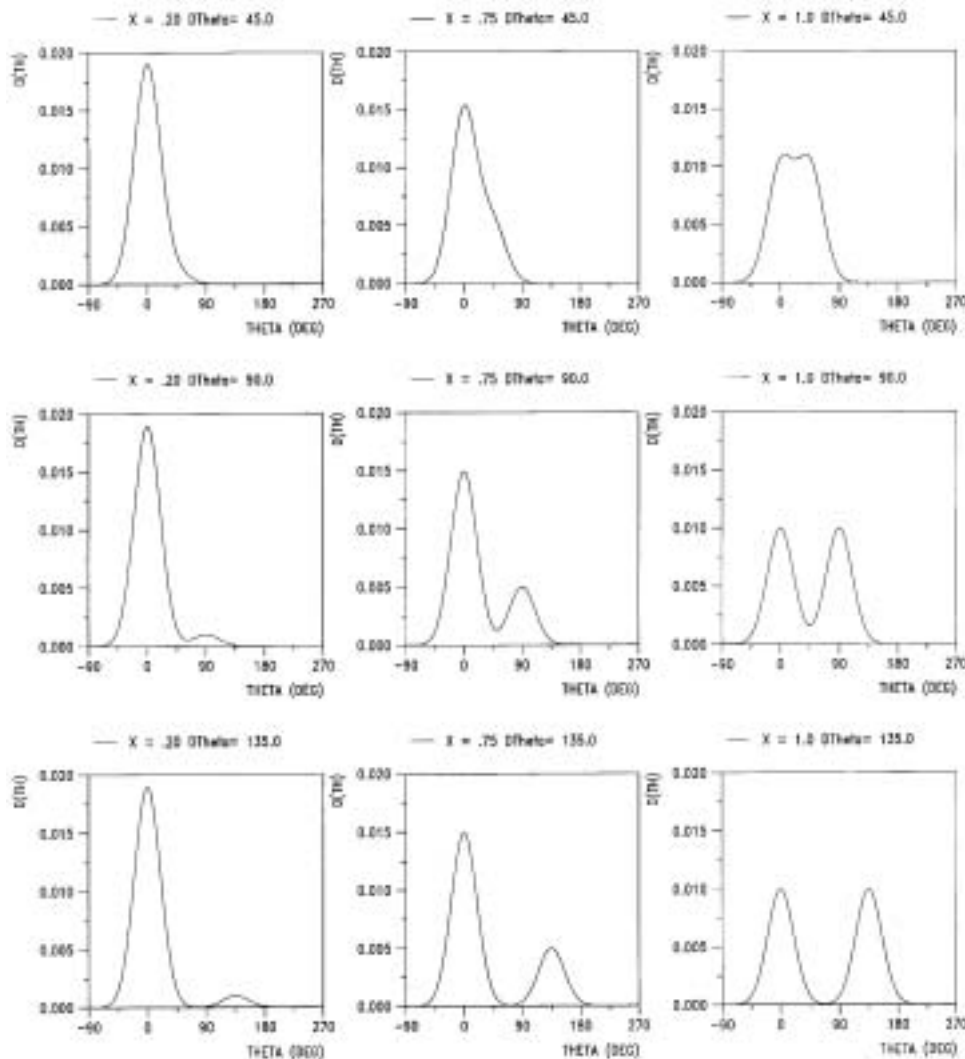


Fig. 3 Examples with bimodal spectrum model (here with  $\sigma_1 = \sigma_{II} = 20$  degrees.)

mately with the exact values:

$$\delta = 1 + 2.75\gamma\xi + 1.8[(1 + 0.1\xi^{-1})/(1 + \gamma\xi^{-1})]/(1 + 0.1\xi^{-1}) \quad (9)$$

where  $\xi \equiv (x)^{-1/2} - 1$ . This relation uniquely combines  $\delta$ ,  $\gamma$  and  $x$ . The “start value” 2.80 for  $\delta$ , at  $\gamma = 0$ , is reasonably close to the value 3.0 expected for uni-modal Gaussian spectra. In fact, for unimodal symmetric cases ( $x = 0$ , not included in the figure), the skewness is zero and the computed kurtosis is close to 3.0 for narrow spectra, while it decreases to 2.70 for  $\sigma \approx 20 - 30$  degrees (this is consistent with the tail truncation of a linear Gaussian-shaped model).

Not all combinations of  $\delta$  and  $\gamma$  are in fact possible for the two-peaked model eq. (7), and the actual range also depends on the total standard deviation  $\sigma$ . A large peak separation  $\Delta\theta$  in combination with a large  $x$  (that is, a large secondary peak) implies a certain lower limit for  $\sigma$ , even with infinitely narrow peaks. Thus the lower right corner of the plot is impossible, and the restrictions are highest for small  $\sigma$ .

All symmetric spectra, unimodal or bimodal, have zero skewness and fall therefore along the vertical axis of Figure 2. The kurtosis then depends on (decreases with) the width  $\sigma_1$  of each of the components, with 1.0 as its lowest limit for two equally large unidirectional waves (see above). Notice that the cases with a secondary peak from 180 degrees (for example, backward reflections) are interpreted as symmetric by this analysis, regardless of  $x$ . Then small  $x$  gives kurtosis values higher than 2.5 – 3.0, while large  $x$  gives kurtosis between 1 and 2.5.

In general, 180 degree secondary peaks can also be recognized directly from the ratio  $|C_1|/|C_2|$  between the first and the second order Fourier coefficient amplitudes. Values lower than 1 clearly indicate such situations. If we restrict ourselves to the 4-parameter model of eq.(7), the criterion becomes rather  $|C_1|^4/|C_2| < 1$ , as one can easily confirm through eq.(8). With large secondary peaks, this ratio is then close to zero, while smaller peaks give smaller effects. This is further investigated and applied in the next section.

#### A simple bimodal parametric estimation method

The 4-parameter model eq.(7) can be applied in a simple, fast and robust directional spectrum estimation approach based on the 4 known parameters  $\theta_0$ ,  $\sigma$ ,  $\gamma$  and  $\delta$  found from the complex Fourier coefficients  $C_1$  and  $C_2$ . Similar approaches have been considered by Van Heteren (1983) and Benoit (1992). The model certainly has its limitation in identification of all kinds of real spectra, but that will basically be the case with all attempts to extract information with only 4 input parameters. In the following, we describe a method based on the observed behaviour of the  $\gamma - \delta$  relationship from Figure 2. Thus the energy distribution parameter  $x$  (or  $A_{II}/A_I$ ) can be directly found from eq. (9), which leaves the angle separation  $\Delta\theta$  between the two peaks to be finally estimated. (The other two parameters,  $\theta_1$  and  $\sigma_1$ , are then easily determined through  $\theta_0$  and  $\sigma$  which are already directly available from  $C_1$ ). Here we suggest, as one possible method, to extract  $\Delta\theta$  directly

from the skewness  $\gamma$ , since we have found empirically that the following unique and simple relation fits reasonably well with calculated, exact values from eqs.(5) & (8):

$$= 0.225 x (1 - x)^{1/3} (\Delta\theta/\sigma)^3 + [(\sigma - \sigma_0)/\sigma] \cdot [(x - x_0)/x] \quad (10)$$

where  $\sigma_0$ ,  $x_0$  are reference values chosen equal to 20 degrees and 0.5, respectively. Figure 4 shows this through a plot of:

$$\{[\gamma - [(\sigma - \sigma_0)/\sigma] \cdot [(x - x_0)/x]] / [0.225 \cdot x \cdot (1 - x)^{1/3}]\}^{1/3}$$

as a function of  $(\Delta\theta/\sigma)$ ,

for a large variation of  $x$ - and  $\sigma$ - values. Thus for given values of  $\sigma$  and  $x$ , a cubic relation between  $\gamma$  and  $\Delta\theta$  seems to be useful for this spectrum model. (In its present form, the formula works only for  $|\gamma| > 0.2$ . Thus smaller skewness is interpreted as a symmetric case. This could be optimized). With a few exceptions, the actual deviations typically represent 0 – 15% errors in the angular separation  $\Delta\theta$  when normalized with the estimated total spreading  $\sigma$ . The largest deviations occur for large  $\Delta\theta$  (> 90 degrees). Whether this is the most optimal way of estimating  $\Delta\theta$ , can certainly be discussed, but it is very simple, convenient for interpretation and illustration of the problem, and reasonably accurate (within the approximation of this two-peak model). The actual ratio  $\Delta\theta/\sigma$  is highest for sharp peaks ( $\sigma_1 \approx 0$ ) and a small secondary peak ( $x$  is low). Cases with very small  $x$  (that is,  $x \leq 0.1$ , or  $A_{II}/A_I \leq 3\%$ ) are not well reproduced by eq.(10) and is not included in the figure. This could probably be improved by a more sophisticated formulation and is not a basic limitation. An alternative way is to

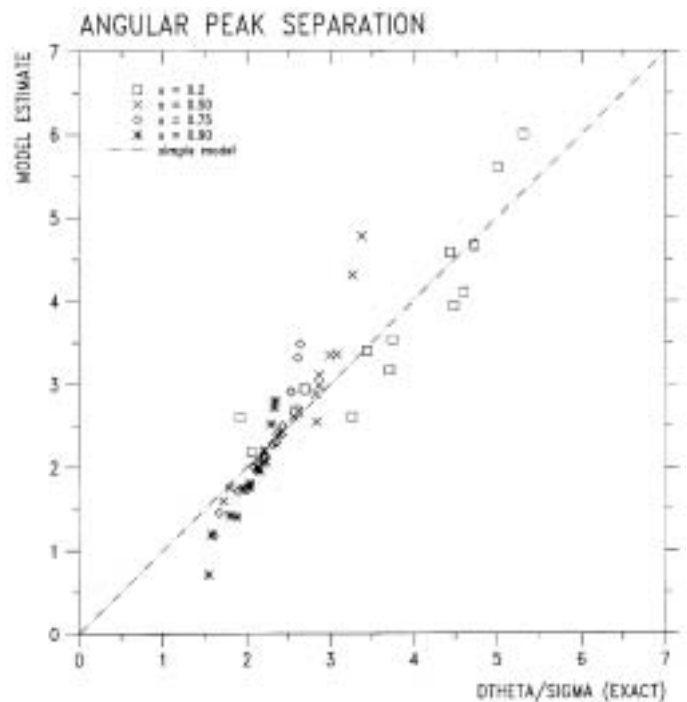


Fig. 4 Correlation between normalized peak separation and estimate based on skewness.

use the ratio  $|C_1|^4/|C_2|$  which depends on  $x$  and  $\Delta\theta$  only (see below).

Notice that spectra with  $\gamma \approx 0$ , that is, symmetric spectra ( $x \approx 1$ ) and / or  $\Delta\theta = 180$  degrees, cannot be included in eq.(10). Information can then be found in other parameters. Kurtosis values equal to 1 means that the spectrum consists of two equal, sharp peaks ( $\sigma_1 \approx 0$ ), while two equal but not so sharp peaks lead to values between 1 and 2.5. Kurtosis values higher than 3 indicates a small secondary peak from 180 degrees. To estimate the angle separation  $\Delta\theta$  in such cases one could consider the ratio  $|C_1|^4/|C_2|$ , which we denote by  $\chi$ . From eq.(8) a simple expression depending on  $x$  and  $\Delta\theta$  only is easily derived for this special Gaussian model:

$$\chi^2 \equiv |C_1|^8/|C_2|^2 = \frac{1}{[1 - 0.5x(1 - \cos(\Delta\theta))]^4 [1 - 0.5x(1 - \cos(2\Delta\theta))]} \quad (11)$$

In the limiting cases with  $\gamma = 0$  (that is, for  $x = 1$  and / or  $\Delta\theta = 180$  degrees, respectively) this reduces to:

$$\chi^2 = (1/16) [1 + \cos(\Delta\theta)]^4 / \cos^2(\Delta\theta) \quad (\text{for } x = 1) \quad (11a)$$

$$\chi^2 = (1-x)^4 \quad (\text{for } \Delta\theta = 180 \text{ degrees}) \quad (11b)$$

which can be used in the estimation of  $\Delta\theta$  or  $x$  based on given  $C_1$ ,  $C_2$  and knowing whether  $\delta$  is lower than 2.5 (leading to eq. (11a)) or higher than 3 (leading to eq.(11b)). In any case, if  $\gamma \approx 0$  and  $\chi^2 \ll 1$ , a condition with  $x \approx 0.75 - 1$  and  $\Delta\theta \approx 180$  degrees is identified, and if  $\chi^2 > 2$ ,  $\Delta\theta$  is close to 90 degrees.

One should keep in mind that our model is a 4-parameter approximation, and that the real condition may be more complex. But used on a more complex situation, it is expected that the parameter  $x$  still can be used as a measure of energy distribution, and not only as an amplitude parameter in a strict 4-parameter model. Real data may also include  $\gamma$ - $\delta$  point-pairs not allowed in this model, in which case an indication of a complex spectrum is given.

Results from use of eqs. (9) – (11) on theoretical examples from the model of eq.(7), including those in Figure 3 plus some more, are shown in Figure 5. We see that the energy distribution parameter  $x$  and the peak separation  $\Delta\theta$  are reasonably well reproduced from the skewness and kurtosis and / or the ratio  $\chi$ . We conclude that by assuming a simplified bimodal spectrum, we are able to determine whether or not there are two peaks, as well as their relative energy and angular separation ( $\Delta\theta$ ). Further investigations are needed to investigate to which extent this depends strictly upon the simplified model, or whether the findings can be used in a broader sense. The limitations in the estimation resolution of  $\Delta\theta$  also need further clarifications. Thus we have found that  $\Delta\theta$  down to 45 degrees can be resolved, while smaller values for  $\Delta\theta$  have not been checked here so far and should be included in future examples. Furthermore, statistical sampling errors due to estimation from finite records may confuse the picture, and an illustration of this is given in the following two chapters.

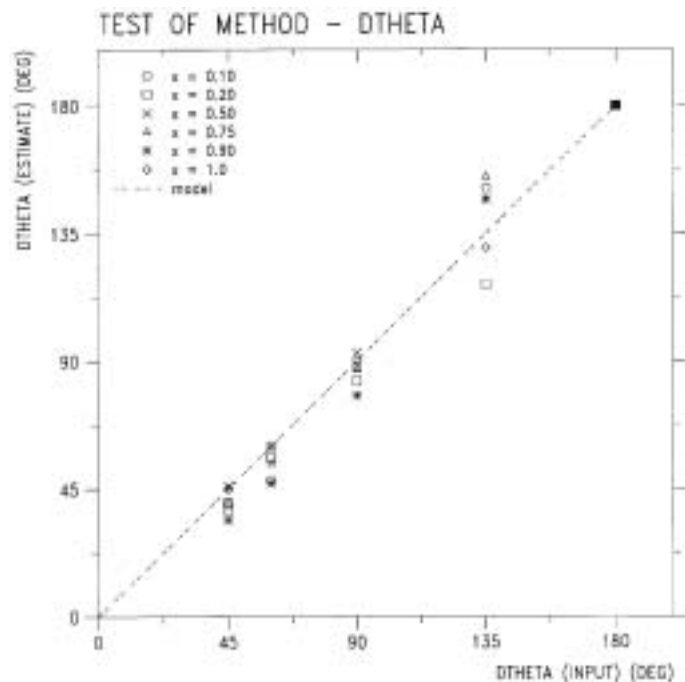
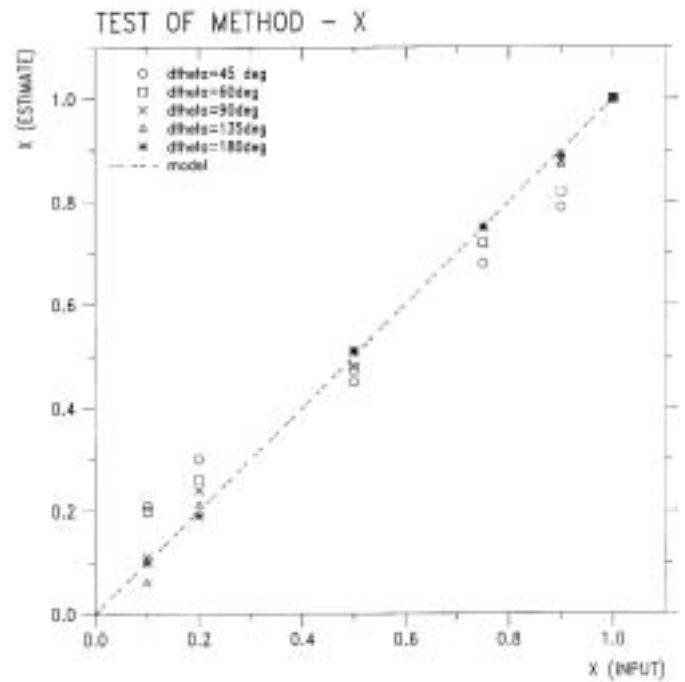


Fig. 5 Estimation of  $x$  (upper) and  $\Delta\theta$  (lower) from skewness and kurtosis, by simple method.

### 3. Statistical sampling errors in a random sea: theoretical background

Assume that the zero-mean multidirectional wave elevation  $\xi(\mathbf{r}, t)$  can be theoretically described as a stationary and homogenous random process in time  $t$  and space  $\mathbf{r}=(r_x, r_y)$ :

$$\xi(\mathbf{r}, t) = \sum_{m=-NF}^{NF} \sum_{n=1}^{ND} \cdot F_{mn} \cdot \exp[j(2\pi f_m t - \mathbf{k}_{mn} \cdot \mathbf{r})] \Delta f \cdot \Delta \theta \quad (12)$$

where  $F_{mn} = |F(f_m, \theta_n)| \cdot \exp[j\phi(f_m, \theta_n)]$  is the complex amplitude of a plane harmonic wave with wave vector  $\mathbf{k}_{mn} = \mathbf{k}(f_m, \theta_n)$ . Here the random characteristics is given by the random phase  $\phi(f_m, \theta_n)$ , which is uniformly distributed in  $\{0, 2\pi\}$  and independent for each frequency-direction combination  $(f_m, \theta_n)$ , while the amplitude  $F$  is a deterministic function in this description. The theoretical (expected) directional distribution of energy is described by the directional frequency spectrum:

$$S(f, \theta) - S(f) \cdot D(f, \theta) = |F(f_m, \theta_n)|^2 \cdot \Delta f \cdot \Delta \theta \quad (13)$$

where  $S(f)$  is the scalar spectrum and  $D(f, \theta)$  is the normalized directional spectrum treated in the previous chapter.

Details and properties of this double-summation model have been described in Stansberg (1998a). When the number of frequencies (NF) and directions (ND) are large (and, correspondingly, the increments  $\Delta f$ ,  $\Delta \theta$  are small), the model is considered to satisfactorily reproduce the statistical properties of a real, random sea realisation in time and space. Applied with too few components, however, non-ergodic properties will occur (Jefferys, 1987). From the experiences in Stansberg (1987; 1998a), it was found that for a 3-hour storm simulation, inverse Fast Fourier Transform (FFT) with 16384 frequencies combined with 100 directions for each frequency, gives reasonable results. This was used in the present simulations, as described in the next section.

Estimation of directional spectra can be considered as the problem of extracting the real  $D(\theta)$  in eq.(12), and its related parameters such as circular moments and Fourier coefficients etc., from a set of finite records of the elevation  $\xi(\mathbf{r}, t)$  or of related quantities. Most conventional directional spectrum estimation procedures are based on the cross-spectra between three or more recorded time series signals derived from the wave elevation, reviewed by Benoit et. al. (1997). This may be the elevation  $\xi(\mathbf{r}, t)$  itself, recorded with a gage array at different locations, or it can be various combinations between the elevation, slope, particle velocities and pressure at a given location. Here we consider the case with wave elevation gage array recordings only, but the principle will be similar also in the other cases. The relation between the directional spectrum and the normalized, complex cross-spectrum (here denoted as the spatial coherence) between two locations at a relative distance  $\Delta \mathbf{r}$  can then be written (Isobe et. al, 1984):

$$S_0(\Delta \mathbf{r}, f) = S(\Delta \mathbf{r}, f) / S(f) = \int_0^{2\pi} D(f, \theta) \exp[-j \mathbf{k}(f, \theta) \cdot \Delta \mathbf{r}] d\theta \quad (14)$$

where  $S(\Delta \mathbf{r}, f)$  is the actual complex cross spectrum and  $S(f)$  is the auto-spectrum of the elevation. The actual records used for the estimation of  $S_0(\Delta \mathbf{r}, f)$  are here random realisations of the process  $\xi(\mathbf{r}, t)$ , and finite in time as well as in space (given by the array size and resolution). This means that although the underlying, theoretical spectrum  $D(f, \theta)$  and its parameters may be deterministic quantities, the estimates will be random variables due to random sampling errors from finite records.

With the use of cross-spectrum based methods, these errors will

arise from random errors in the cross-spectrum estimation. The random characteristics of cross-spectra estimated between the elevations at different locations have been discussed in Stansberg (1998a) based on expressions originally derived in Stansberg (1987). Random sampling errors are shown to increase with the distance between the probes (that is, decrease with the correlation – or spatial coherence – between the signals), and can typically be of the same magnitude as, and also larger than, the cross-spectrum itself except when the relative distances  $\Delta \mathbf{r}$  are clearly smaller than the actual wavelengths. See the example in Figure 6, from a numerical example with a 4.5 hours sea state duration. On the other hand, the sensitivity effects on the directional estimates are stronger when the coherence is high. The spectral smoothing, or averaging, also plays an important role in the elimination of such errors from the estimates. This is equivalent to the actual length of the records. Durations corresponding to several hours, full scale, are considered to be favourable for a stable estimate. In practice, we can then make cross-spectrum estimates averaging over 50 – 100 neighbouring frequencies.

For the actual circular moments and Fourier coefficients of the directional spectra, expressions can then be derived based on eq.(14) or similar expressions, as formulated by many authors throughout the last decades, and reviewed by Benoit et. al. (1997). Parameters such as the directional mean, spreading, skewness, kurtosis and derived parameters can then be estimated, as described earlier in this paper. In the following, the resulting sampling errors in these parameters are investigated and illustrated through a numerical simulation case study.

#### 4. Numerical simulation examples

Results from a numerical case study are presented for the illustration of typical statistical errors in estimates for the directional parameters  $\theta_0$ ,  $\sigma$ ,  $\gamma$  and  $\delta$ . A short description of the actual case study problem is given first.

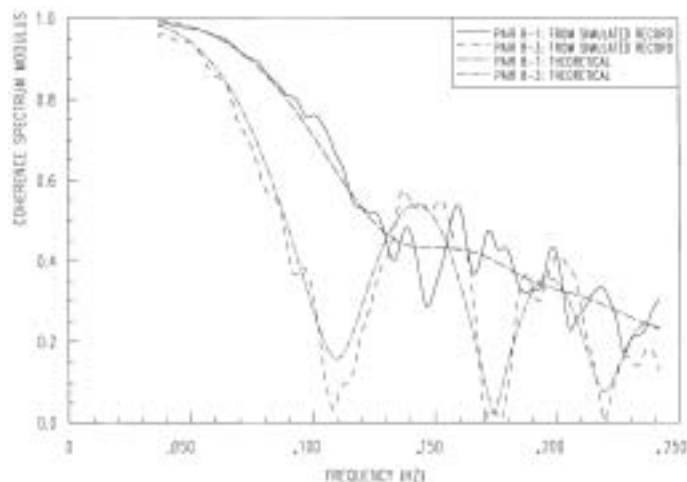


Fig. 6 Example on a coherence function (i.e. the modulus of a normalized cross-spectrum) estimate between random numerically simulated records (corresponding to 4.5 hours), compared to theoretical values. Wave staff spacing: 50m.

### Random wave simulations

Data records from an earlier numerical study (Stansberg, 1998a) are used. Wave elevation records are numerically simulated at the specified locations of the array (defined in the next section) based on the double-summation technique in eq.(11). This technique generates records that simulate the statistical characteristics of random realisations of a given sea state, provided that a large number of frequencies and directions are used. Here we use  $NF = 16384$  equidistant frequencies and  $ND = 100$  directions. Inverse Fast Fourier transform (FFT) is used for the summation over frequencies  $f$ , which makes the computation time reasonably low. With a sampling interval of 0.5 seconds, this gives a total record duration of 4.5 hours, which is reasonably long and considered to be sufficient for obtaining stable estimates of cross spectra. Each 4.5-hours sea state is run as 6 different realisations, for the study of variability. For one of the conditions, the present analysis is also done for a smaller part (1 hour) of the time series, to see the effect from the duration on the statistics.

A JONSWAP wave spectrum with  $H_s=10m$ ,  $T_p=15s$ ,  $\Gamma=2$  was used in the simulations. The following directional spectra were included (see also Figure 7):

- Sea State 1:  $D(\theta) \propto \cos^2\theta$
- Sea State 2:  $D(\theta) \propto \cos^2(\theta+60) + 1.4\cos^{20}(\theta-30)$
- Sea State 3:  $D(\theta) \propto \cos^{20}\theta$
- Sea State 4:  $D(\theta) \propto \cos^{20}(\theta+22.5) + \cos^{20}(\theta-22.5)$

### Estimation of directional Fourier coefficients with circle-shaped array

In these illustrating examples, wave elevation records obtained with a circularly shaped wave gage array are used. The array has

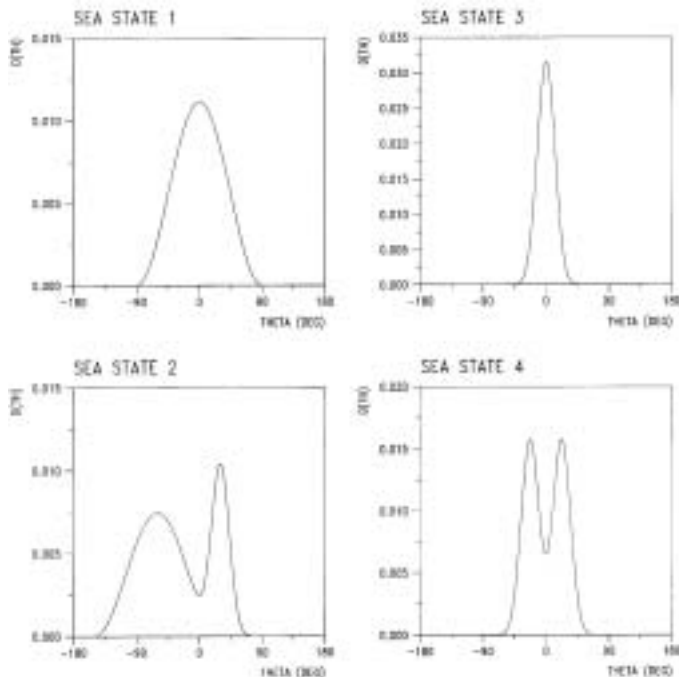


Fig. 7 Directional spectra in numerical case study.

a radius  $R$ , and  $N$  points on the circle, plus one in the centre. Such gage arrays are mainly used in laboratory situations, so this can be considered as the numerical simulation of a model test case. All quantities will, however, be given in full scale values. Other types of input data could certainly also be used for the purpose of this study. It was, however, convenient to use these data already available and used in earlier investigations.

From the array recordings, coherence estimates (i.e. normalized complex cross spectra) for point-pairs distributed on a number of different circles can be obtained. Eqs. (1) and (14) can be combined to express the complex Fourier coefficients  $C_m$  based on measured, normalized cross-spectra  $S_0$  for the different point-pairs  $\Delta\mathbf{r}_n$ : Using all possible ( $=2N$ ) combinations with the same absolute distance  $|\Delta\mathbf{r}|$  but different angles  $\alpha_n = \arctg(\Delta r_{ny}/\Delta r_{nx})$ , we get (Stansberg & Ishida, 1989):

$$C_m = [1/(2\pi J_m(z))] \cdot (1/2N) \cdot \sum_{n=1}^{2N} S_0(|\Delta\mathbf{r}|, \alpha_n) \cdot \exp[-jm(\alpha_n + \pi/2)] \quad (15)$$

where  $z = k \cdot |\Delta\mathbf{r}|$ , and  $J_m$  is the Bessel function of 1st kind and order  $m$ . The direction  $\alpha_n$  is here given in radians. The summation over  $n$  is done all over the circle. Note that  $S_0(|\Delta\mathbf{r}|, \alpha_n) = S_0^*(|\Delta\mathbf{r}|, \alpha_{n+N})$  (\* here means complex conjugate), and that choosing  $N$  as an odd number is optimal. In principle, coefficient orders  $m$  up to  $N$  can be estimated this way, but in practice the maximum order will often be lower. This is partly due to the above mentioned statistical variability in  $S_0$ , which induces sampling errors in  $C_m$ , and partly due to low values that can occur in the Bessel functions. For long waves ( $k|\Delta\mathbf{r}| < 1$ ), only  $C_1$  and  $C_2$  can be found.

The capability of the method has been demonstrated through numerical examples in Stansberg (1998b). Resulting estimates for  $C_m$  showed very good correspondence with the specified (theoretical) values, when cross-spectra without sampling errors were used as input. With sampling errors included in  $S_0$  (Stansberg, 1998a), random variations also occur in the estimates for  $C_m$ , as expected. The simulations from the latter reference are also made use of in the examples of the present work, but now we focus only on the influence on some of the derived directional parameter estimates discussed in the previous chapter. Thus we need only to include complex Fourier coefficients  $C_m$  with orders 1 and 2. (Notice that if the simulated estimate  $C_2$  happens to fall outside the permitted range given by eq.(6a), it is adjusted to just fall inside. Otherwise the kurtosis becomes less than 1, which is not physical). The actual array used here is a 8-gage array ( $N = 7$  points on the circle plus one in the center), with radius  $R = 50m$  (full scale), as illustrated in Figure 8.

### Results with discussion

Directional parameters based on  $C_1$  and  $C_2$  estimated at the peak frequency ( $f = 0.066Hz$ ), are presented in Figures 9 & 10. Simulated results for the mean direction  $\theta_0$ , the total spreading  $\sigma$ , the skewness  $\gamma$  and the kurtosis  $\delta$  are shown. The statistical variability

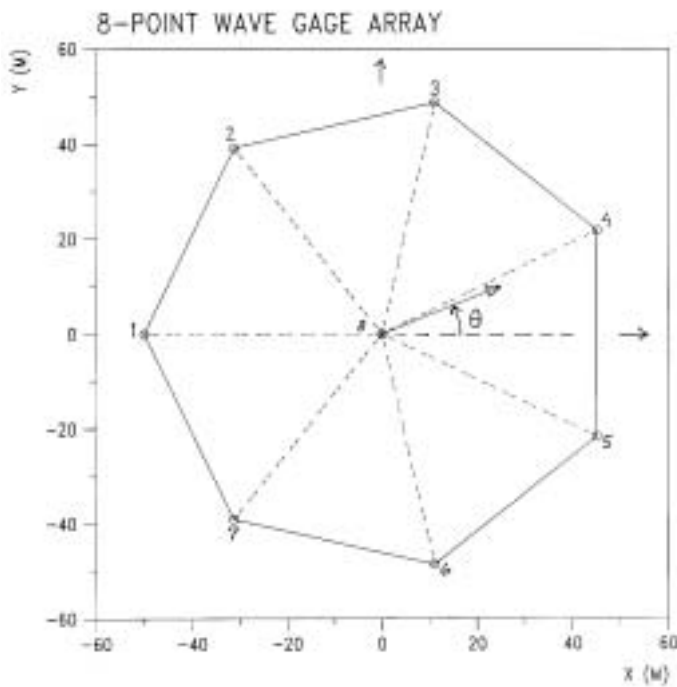


Fig. 8 Circular wave staff array used in numerical case study.

ity is investigated through 6 different realisations for each of the 4 sea states of 4.5 hours duration. Also included in the plots are results for shorter runs, as well as the theoretically expected values.

We see that for the three symmetric cases (1,3 & 4), the estimated mean direction is reasonably stable and close to the target, with up to a few degrees of variation. For case 2, there is a larger scatter – typically  $\pm 3 - 4$  degrees, and even more for the shorter records (as expected). This may in parts be due to the larger spreading angle, as well as the bi-modality. Case 2 also has a bias in the average estimate, although this bias was not seen in a check with theoretical cross-spectra used as input.

For the estimated spreading angle the scatter is small in all cases, only a few degrees of variation, and except from case 3 the averages are close to their targets. The scatter is hardly any larger for the short 1-hours duration, which may be a little surprising. However, one should remember that the influence from cutting the duration down from 4.5 to 1 hours results in an expected increase of a factor of 2 in the variability of cross-spectra. With only 6 realisations, this increase may not necessarily always be distinct in the results. It is also likely that the variability in cross-spectra are not linearly transferred to the actual parameters. The bias for case 3 may be related to the actual estimation procedure – one must also remember that since  $|C_1|$  is very close to 1 in this narrow-spectrum case, the estimates are extremely sensitive to small variations in its value.

The skewness, which in these cases are around zero, shows variations in the range  $\pm 0.20$  around their expected values. A larger deviation is seen for case 3, but here the total spreading is small so the practical effect is also small. We see that the expected skewness in case 2, although small, is not reproduced in the averages, and this could be seen in connection with the bias in the mean direction. Again, the 1-hour data do not seem to give any

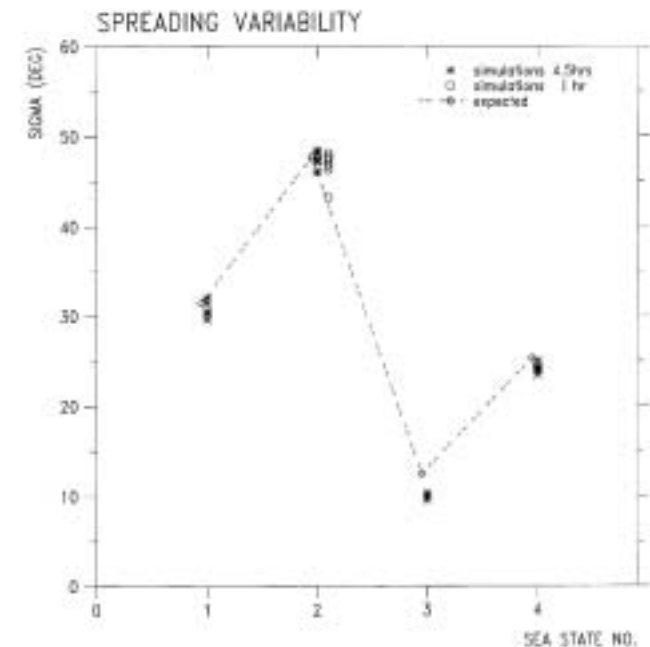
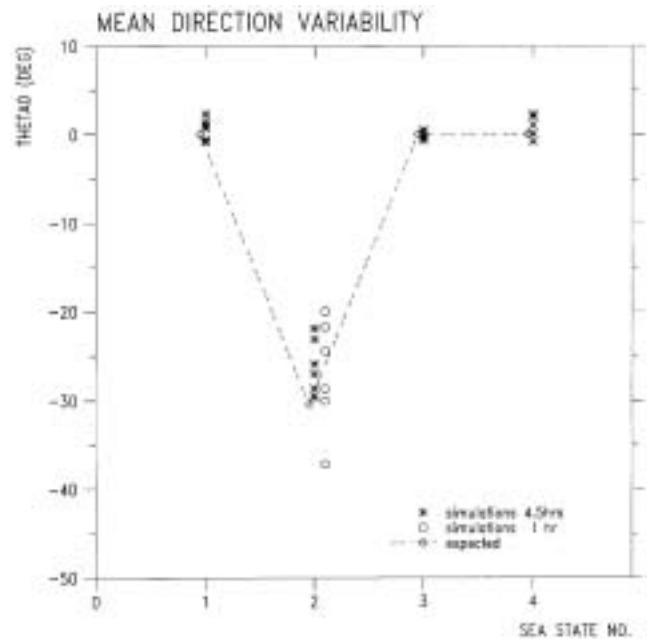


Fig. 9 Accuracy and statistical variability of estimates from random wave simulations. Upper: mean direction  $\theta_0$ ; Lower: total spreading  $\sigma$ .

significantly higher scatter. As commented for  $\sigma$  above, the reason may be partly too few realisations, and partly that the scatter in  $\gamma$  does not follow directly the trend of the cross-spectrum..

Kurtosis values in these examples are all in the range between 1 and 2.5, which means that the spectra are either unimodal or almost symmetric multimodal. With smaller secondary peaks in the input spectra, kurtosis values would have been higher. This agrees with the input spectra, Figure 7, except from case 2. But measured in energy, also case 2 has two peaks of approximately equal size, so the analysis is still consistent in that sense. For case 1, the

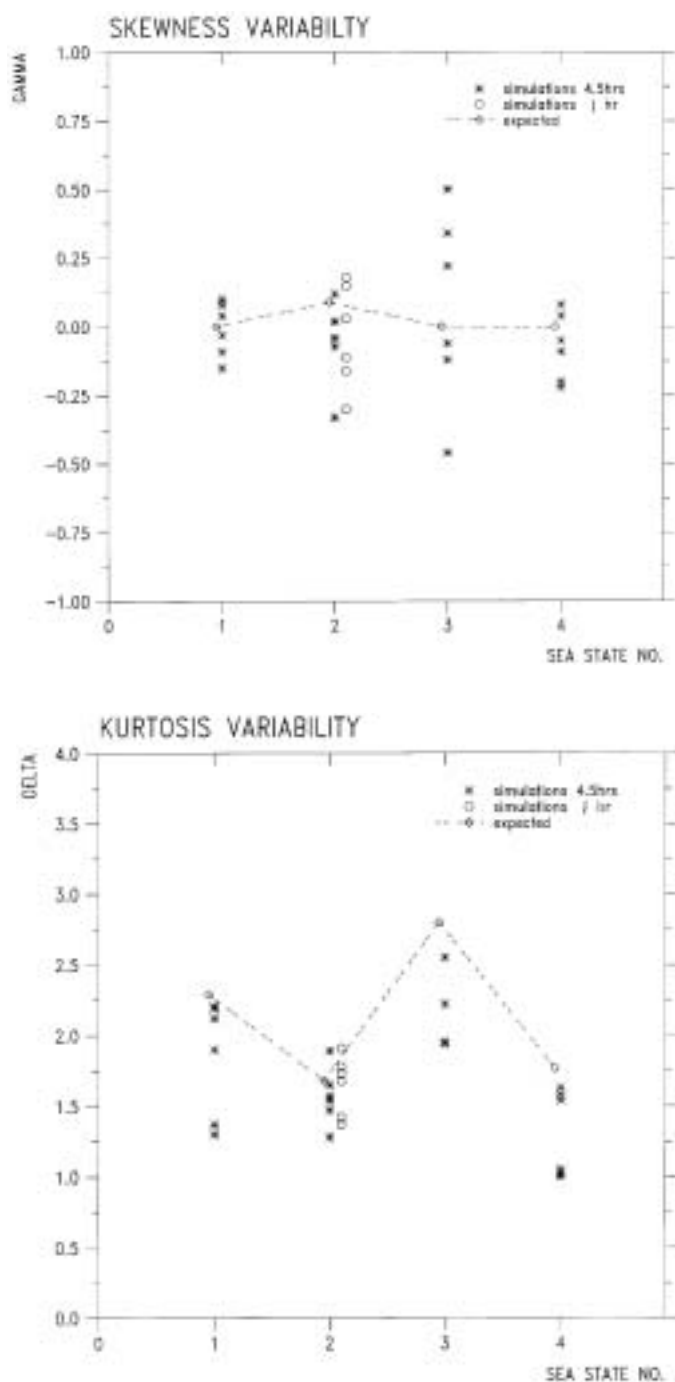


Fig. 10 As Figure 9, but for skewness (upper) and kurtosis (lower).

kurtosis estimates may seem low, since a unimodal symmetric spectrum is expected to have values around 2.5 – 3.0. The reason is probably that a  $\cos^2\theta$ -spectrum is not exactly Gaussian, and the case is in fact very close to the limit of eq.(6). Therefore the analysis will suggest two equal peaks (which can look like a single-peak spectrum when the peaks are close). The observed scatter in the kurtosis is typically  $\pm 0.40$  in all cases.

The ratio  $\kappa^2$  from eqs.(11-11b) has also been computed, although not shown in the figures. It shows very high values for sea state 2, which indicates two approximately equal peaks separated by 90 degrees, and that is reasonably consistent with the input (if we measure the peaks by their energy). For sea state 4, it also shows values somewhat higher than 1. Together with the low kurtosis

values combined with zero skewness, which indicates two approximately equal peaks, this gives an estimate for  $\Delta\theta$  at approximately 45 – 60 degrees. This is also close to the target.

The results shown give an indication of the accuracy and typical statistical errors to be expected in directional parameter estimation, for a limited set of spectrum types. The variability in other parameters such as the bimodal energy distribution  $\alpha$  and the peak separation  $\Delta\theta$  from chapter 2 has not been studied so far, but is a task for further development. Investigations of a larger range of directional spectrum combinations, such as those in Figure 3 and others, should also be included in future work in order to check the variability in cases with higher skewness and kurtosis.

### 5. Concluding remarks

By use of a simple four-parameter bimodal spectrum model, the properties of directional parameters derived from the first two complex Fourier coefficients have been investigated, including the mean direction, standard deviation, skewness and kurtosis. It is found that in a domain defined by the skewness and kurtosis, cases with small secondary peaks are clearly distinct from cases with two approximately equal peaks. This is used to suggest a simple and robust parametric bimodal estimation method, where an empirically observed cubic relationship between the skewness and the angular peak separation is also applied. Although a 4-parameter two-peak model is not always an accurate description of a real case, it seems to be a reasonable way of using the limited information available from a 4-parameter input. Thus in addition to the two “standard” parameters – the mean direction and total spreading, the method also provides information on the relative energy of a possible secondary peak, and the angular separation. For further details, information from higher Fourier coefficient orders would be needed. Moreover, the method should be tested further on other types of distributions than those applied in the present study.

The directional resolution of a peak separation of 45 degrees or less is in general expected to be moderate or poor with only 4 input parameters. However, it is seen from the present results that the method can work reasonably well also in down to 45 degrees. Smaller separations have not been checked in this study, and should be investigated. The “easiest” cases are seen to be exactly 90 or 180 degrees of separation, for which particular or singular behaviours can be observed for certain parameters.

The statistical variability (or “errors”) in the directional parameters, due to finite records, has been illustrated through a numerical case study. Long records are used, corresponding to 4.5 hours full scale. In these examples, only a limited set of spectra, with low skewness and kurtosis values, have been considered, and further numerical investigations should be made to cover a larger range. It is observed that the total spreading estimate is quite stable, while the error in mean direction increases with the spreading (and possibly also depends on the shape of the spectrum). For the skewness and the kurtosis, the typical variation is in the range  $\pm 0.20$  and  $\pm 0.40$ , respectively. The corresponding effect on the actual directional peak separation and the energy distribution is not considered in particular, but it is expected not to be dramatic.

Thus the main structure in the spectra seems to be identified, but this subject should be further investigated.

It is also seen that for the skewness and kurtosis, there is not any clearly larger scatter in shorter (1-hours) records. This may be explained by a combination of too few records (6 realisations for each condition), and a complex relation between the statistical variability in the cross-spectrum and in those two parameters. From these results, we may also conclude that for the estimation of the first 4 parameters, it is probably not necessary to run such long records – 1 hour may be fine. But this should be clarified in further work. For finer resolution studies, however, where higher Fourier coefficients (or similar type of information from other types of analysis) is included, the record duration is likely to be more important.

## 6. References

- BENOIT, M. (1992), 'Practical Comparative Performance Survey of Methods Used for Estimating Directional Wave Spectra from Heave-Pitch-Roll Data', *Proceedings, Vol. 1, 23<sup>rd</sup> Int. Conf. on Coastal Engineering*, Venice, Italy, pp. 62 – 75.
- BENOIT, M., FRIGAARD, P. and SCHÄFFER, H.A. (1997), 'Analysing Multidirectional Wave Spectra: A Tentative Classification of Available Methods', *Proceedings, IAHR Seminar on Multidirectional Waves and their Interaction with Structures*, 27<sup>th</sup> IAHR Congress, San Francisco, Cal., USA, pp. 131 – 158.
- BESNARD, J-C. and BENOIT, M. (1994), 'Representative Directional Wave Parameters – Review and Comparison on Numerical Simulations', *Proceedings, Vol. 2, International Symposium: Waves – Physical and Numerical Modelling*, Vancouver, Canada, pp. 901 – 910.
- BORGMAN, L. (1969), 'Directional Spectra Models for Design Use', *Proceedings, Offshore Technology Conf.*, Houston, TX, USA, pp. 721 – 746.
- BRIGGS, M.J. (1997), 'IAHR Working Group on Multidirectional Waves : An Historical Overview', *Proceedings, IAHR Seminar on Multidirectional Waves and their Interaction with Structures*, 27<sup>th</sup> IAHR Congress, San Francisco, Cal., USA, pp. 1 – 13.
- BURG, J.P. (1975), 'Maximum Entropy Spectral Analysis', Dr. Thesis, Stanford University, Calif., USA.
- FRIGAARD, P., HELM-PETERSEN, J., KLOPMAN, G., STANSBERG, C.T., BENOIT, M., BRIGGS, M.J., MILES, M., SANTAS, J., SCHÄFFER, H.A. and HAWKES, P. (1997), 'IAHR List of Sea State Parameters, An Update for Multidirectional Waves', *Proceedings, IAHR Seminar on Multidirectional Waves and their Interaction with Structures*, 27<sup>th</sup> IAHR Congress, San Francisco, Cal., USA, pp. 15 – 24.
- HASHIMOTO, N. (1997), 'Analysis of the Directional Wave Spectrum from Field Data', *Advances in Coastal and Ocean Engineering, Vol. 3*, Ed. P.L.F. Liu, World Scientific, Singapore.
- ISOBE, M., KONDO, K. and HORIKAWA, K. (1984), 'Extension of MLM for Estimating Directional Wave Spectrum', *Proc., Symp. on Description and Modelling of Directional Seas*, DHI, Copenhagen, Denmark.
- JEFFERYS, E.R. (1987), 'Directional Seas Should be Ergodic', *Applied Ocean Research, Vol. 9* (4), pp.186-191.
- KOBUNE, K. and HASHIMOTO, N. (1986), 'Estimation of Directional Spectra from the Maximum Entropy Principle', *Proc., 5<sup>th</sup> OMAE Conf., Vol. 1*, Tokyo, Japan, pp.80-85.
- KROGSTAD, H.E. and BARSTOW, S.F. (1999), 'Directional Distributions in Ocean Wave Spectra', *Proceedings, Vol. III, the 9<sup>th</sup> ISOPE Conf.*, Brest, France, pp. 79 – 86.
- KUIK, A.J., VAN VLEDDER, G.Ph. and HOLTHUIJSEN, L.H. (1988), 'A Method for the Routine Analysis of Pitch-and Roll Buoy Wave Data', *Journal of Phys. Ocean., Vol. 18*, pp. 1020 – 1034.
- LONGUET-HIGGINS, M.S., CARTWRIGHT, D.E. and SMITH, N.D. (1963), 'Observations of the Directional Spectrum of Sea Waves Using the Motions of a Floating Buoy', *Ocean Wave Spectra*, Prentice-Hall, pp. 111 – 136.
- MARDIA, K.V. (1972), *Statistics of Directional Data*, Academic Press, London, U.K.
- NWOGU, O.U., MANSARD, E.P.D., MILES, M.D. and ISAACSON, M. (1987), 'Estimation of Directional Wave Spectra by the Maximum Entropy Method', *Proc., IAHR Seminar on Wave Generation and Analysis in Laboratory Basins*, Lausanne, Switzerland.
- NWOGU, O.U. (1989), 'Maximum Entropy Estimation of Directional Wave Spectra from an Array of Wave Probes', *Applied Ocean Research, Vol. 11*, No. 4, pp. 176-193.
- STANSBERG, C.T. (1987), 'Statistical Properties of Directional Sea Measurements', *ASME OMAE Journal, Vol. 109*, No. 2, pp. 142 – 147.
- STANSBERG, C.T. (1998a), 'Modelling and Analysis of Multidirectional Waves: Statistical Variability and Directional Resolution', *Proceedings, RealSea '98 – International Workshop on Modelling of Ocean Environments in Wave & Current Basin*, KRISO, Teajon, Korea, pp. 22 – 39.
- STANSBERG, C.T. (1998b), 'On the Fourier Series Decomposition of Directional Wave Spectra', *Proceedings, Vol. III, the 8<sup>th</sup> ISOPE Conference*, Montreal, Canada, pp. 227 – 234.
- STANSBERG, C.T. and ISHIDA, S. (1989), 'Directional Spectrum Estimation by Means of a Circular Wave Gauge Array', *Proceedings, Vol. C, 23<sup>rd</sup> IAHR Congress*, Ottawa, Canada, pp. C251 – C258.
- VAN HETEREN, J. (1983), 'Estimation of Multi-Modal Directional Wave Spectra from Tri-Orthogonal Measurements', *Coastal Engineering, Vol. 7*, pp. 205 – 231.